

P. Sivonen, S. Kangasmaa, and A. Pärssinen, A SiGe RF front-end with on-chip VCO for a GPS receiver, in Proceedings of the European Solid-State Circuits Conference, pp. 435-438, Florence, Italy, Sep. 2002.

© 2002 IEEE

Reprinted with permission.

This material is posted here with permission of the IEEE. Such permission of the IEEE does not in any way imply IEEE endorsement of any of Helsinki University of Technology's products or services. Internal or personal use of this material is permitted. However, permission to reprint/republish this material for advertising or promotional purposes or for creating new collective works for resale or redistribution must be obtained from the IEEE by writing to [pubs-permissions@ieee.org](mailto:pubs-permissions@ieee.org).

By choosing to view this document, you agree to all provisions of the copyright laws protecting it.

## A SiGe RF Front-End with On-Chip VCO for a GPS Receiver

P. Sivonen, S. Kangasmaa, A. Pärssinen  
 Nokia, Helsinki, Finland  
 pete.sivonen@nokia.com

### Abstract

A GPS direct conversion RF front-end with on-chip VCO fabricated in 0.35 $\mu\text{m}$  SiGe BiCMOS technology is presented. The properties of inductively degenerated common-emitter LNA and resistively degenerated Gilbert downconversion mixer are examined. The approximative equations for the front-end DSB-NF and IIP3 are given. By applying the derived formulas, the front-end performance can be readily estimated and optimized. The implemented RF front-end has a voltage conversion gain of 25.8 dB, DSB-NF of 2.7 dB, IIP3 of -14.5 dBm and IIP2 of +26 dBm. The 3.15 GHz VCO has a phase noise of -99 dBc/Hz at 100 kHz offset. The front-end draws 15.3 mA from a 2.7 V supply.

### 1. Introduction

As GPS receivers become common in portable mass products, the power consumption, cost, size, and yield of the receiver parts become critical. Here, a low-power, robust, and high-performance 0.35 $\mu\text{m}$  SiGe RF front-end for a GPS receiver is presented. The on-chip RF section of the receiver (Fig. 1) consist of an LNA, I and Q mixers, LO buffers, divide-by-two quadrature generator, and double-frequency VCO. In order to reject the interference from substrate or supply, balanced circuits are employed. The receiver is mounted in a QFN package.

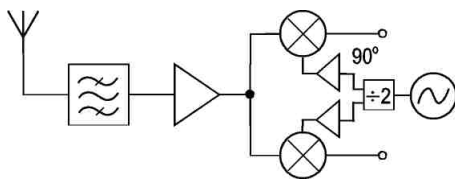


Figure 1. RF front-end of GPS homodyne receiver.

### 2. LNA

The LNA is based on the most commonly used topology i.e. inductively degenerated common-emitter amplifier as shown in Fig. 2. The preselection filter with single-ended input and balanced output transforms the single-ended signal differential for LNA, thus, omitting the need for additional balun. The LNA input impedance at the frequency of operation was selected to be 50  $\Omega$  differential instead of 100  $\Omega$ . The parasitic package capacitance  $C_p$

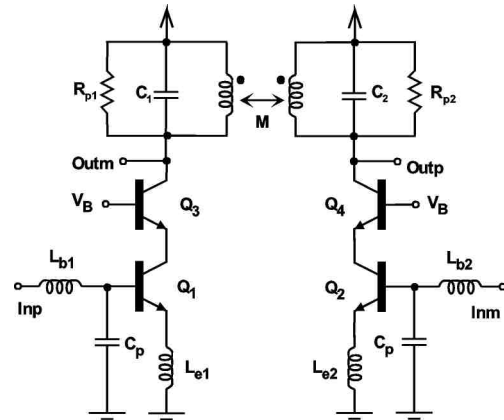


Figure 2. Schematic of LNA.

at the transistor base, within same order of magnitude as  $C_\pi$ , makes it difficult to realize an input impedance larger than 50  $\Omega$  without wasting power or using large emitter inductance. The impedance level could be increased also by a passive impedance transformation network, but this would require extra components complicating the design and increasing the cost.

The amplifier is biased with PTAT base current driven through 20 k $\Omega$  resistors used to isolate the bias circuit from the signal path. The sizes of the input devices  $Q_1$  and  $Q_2$  are selected to be 4 x minimum size in order to ensure that the contribution of the base resistance  $r_b$  to the amplifier noise figure is negligible. The devices  $Q_1$  and  $Q_2$  are biased at the collector current of 1.1 mA each and then the required emitter inductance to realize an input impedance of 50  $\Omega$  is about 1.1 nH. Finally, in order to series resonate the input impedance at 1.575 GHz, the (external) base inductors of about 8.2 nH are needed.

If the noise contributions of the cascode transistors are neglected and perfect input matching ( $R_{in} = R_s$ ) is assumed, the LNA noise figure at the resonance frequency  $\omega_0$  can be approximated as

$$NF_{LNA} = 1 + \frac{R_{lb}}{R_s} + \frac{r_b k^2}{R_s} + \frac{g_m R_s}{2\beta_0 k^2} + \frac{k^2}{2g_m R_s \beta_0} \left(\frac{\omega_T}{\omega_0}\right)^2 + \frac{g_m R_s}{2k^2} \left(\frac{\omega_0}{\omega_T}\right)^2 + \frac{4R_s}{R_L k^2} \left(\frac{\omega_0}{\omega_T}\right)^2 \quad (1)$$

where  $\omega_T \approx \frac{g_m}{C_\pi}$  and  $k = \frac{C_\pi}{(C_p + C_\pi)}$ . For the designed LNA,  $R_{lb} = 2.2 \Omega$ ,  $r_b = 5.0 \Omega$ ,  $R_s = 25 \Omega$ ,  $k = 0.5$ ,  $g_m = 43 \text{ mS}$ ,  $\beta_0 = 88$ ,  $C_\pi = 575 \text{ fF}$  and  $R_L = 80 \Omega$ .

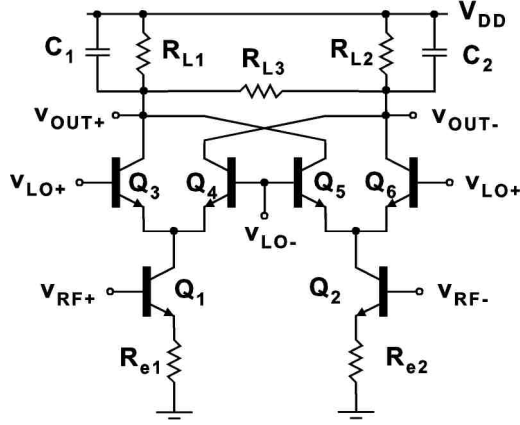


Figure 3. Schematic of downconversion mixer.

Substituting data into Eq. (1) gives

$$NF_{LNA} = 1 + \frac{2.20}{25} + \frac{1.20}{25} + \frac{2.46}{25} + \frac{0.98}{25} + \frac{2.26}{25} \approx 1.35 \text{ dB}. \quad (2)$$

Simulations predict 1.54 dB with cascode transistors making some contribution. The largest contributions in this case are seen to be the base shot noise  $i_b^2$  of the device, the equivalent parallel load resistance  $R_L$  and the series resistor  $R_{lb}$  of the base inductor  $L_b$ , respectively. The noise contributions of the cascode devices are minimized by using the minimum area devices because then the capacitances at their emitters are minimized [1].

A tuned load peeks the gain of the amplifier at 1.575 GHz. The load comprises a 7 nH differential inductor resonating with the parallel capacitance of 0.95 pF, realized with  $C_1 = C_2 = 1.9$  pF, and parasitics. The parallel resistors  $R_{pi}$  set the LNA voltage gain to 20.5 dB. The LNA and mixers are ac-coupled with the 4 pF capacitors.

### 3. Downconversion Mixer

The downconversion mixers are implemented as modified Gilbert cells with resistively degenerated common-emitter RF input stages as shown in Fig. 3. To relax the linearity requirements of the following baseband block, the output of the mixer consist of a first-order RC low-pass filter. The resistors  $R_{L1} - R_{L2}$  are used to set the output common-mode level. The mixer voltage gain can be tuned to the desired value by tuning the resistance  $R_{L3}$ .

If the noise contribution of the switching quad is neglected and the mixer commutation is assumed square-wave like [2], the mixer DSB-NF can be approximated as

$$NF_{DSB} = \frac{\pi^2}{8} \left( 1 + \frac{r_b}{R_{out1}} + \frac{g_m(R_{out1} + R_e)^2}{2R_{out1}\beta_0} \right) + \frac{1}{2g_m R_{out1}} + \frac{R_e}{R_{out1}} + \frac{2(1 + g_m R_e)^2}{g_m^2 R_L R_{out1}} \quad (3)$$

where  $R_{out1}$  is the single-ended LNA output impedance. Figure 4 shows the DSB-NF given by Eq. (3) as a function of collector bias current  $I_c$  with emitter degeneration

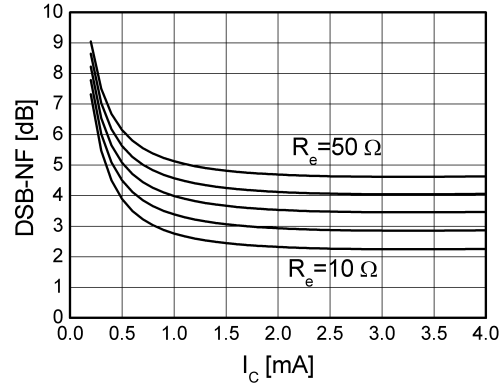


Figure 4. DSB-NF given by Eq. (3).

resistance values  $R_e = 10, 20, 30, 40, 50 \Omega$ . The component values used are  $r_b = 5.0 \Omega$ ,  $R_{out1} = 80 \Omega$ ,  $\beta_0 = 88$  and  $R_L = 190 \Omega$ .

The linearity of the front-end is dominated by the mixer and the main source of mixer nonlinearity is the input RF stage. Thus, the odd-order nonlinearity of the mixer can be examined by using the results derived in [3], in which the high-frequency nonlinearity equations in Volterra series for the degenerated common-emitter amplifier stage are derived. Using two input signals of the same amplitude  $V_s$  at frequencies  $\omega_a$  and  $\omega_b$ , the magnitude of the input-referred  $IM_3$  products at frequencies  $(2\omega_a - \omega_b)$  and  $(2\omega_b - \omega_a)$  of the mixer RF input stage is given by [3]

$$|IM_3| \approx \left| \frac{A_1(s)}{I_c} \right|^3 \left| \frac{V_T}{4} [1 + sC_{je}Z(s)] \left\{ -1 + \frac{A_1(\Delta s)}{g_m} + \frac{A_1(2s)}{2g_m} [1 + 2sC_{je}Z(2s)] \right\} \right| |V_s|^2 = |K(s)| |V_s|^2 \quad (4)$$

where  $Z(s) = Z_b(s) + R_e$ ,  $Z_b$  is the impedance at the base, and  $A_1(s)$  is the Volterra series coefficient. If it is assumed that the IIP3 of the whole front-end is mainly determined by the mixer linearity, the IIP3 in dBm of the front-end is given by

$$IIP3 = 10 \log \left( \frac{2}{A_v^2 \cdot |K(s)| \cdot R_s \cdot 1mW} \right) \quad (5)$$

where  $A_v$  is the LNA voltage gain (20.5 dB). Figure 5 shows the IIP3 of the front-end given by Eq. (5) as a function of  $I_c$  with  $R_e = 10, 20, 30, 40, 50 \Omega$ .

In this design, the mixer was biased with the collector current of 1.3 mA and the emitter degeneration resistance of  $30 \Omega$  was used. With these parameters the designed mixer has a low contribution to the front-end noise figure and the linearity of the front-end is sufficient with a low-power consumption. By substituting the data of the mixer designed in this work to Eq. (3) gives

$$NF_{DSB} = \frac{\pi^2}{8} \left( 1 + \frac{5.0}{80} + \frac{3.6}{80} + \frac{9.5}{80} + \frac{30.0}{80} + \frac{25.2}{80} \right) \approx 3.7 \text{ dB}. \quad (6)$$

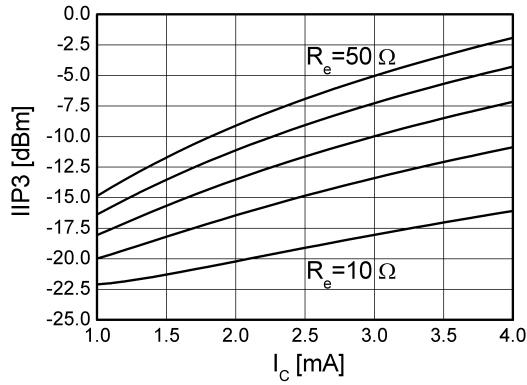


Figure 5. IIP3 of front-end given by Eq. (5).

Simulations predict 4.1 dB with the switching quad making some contribution. In this case, the largest contributions to the mixer noise figure are seen to be the  $R_e$ , the equivalent load resistance  $R_L$  and the collector shot noise  $i_c$  of the RF input device, respectively.

The DSB-NF of the whole front-end is given by [4]

$$NF = NF_{LNA} + 2 \cdot \frac{(NF_{DSB} - 1)}{G_a} \quad (7)$$

where the  $G_a$  is the LNA available power gain given by

$$G_a = \frac{A_v^2 R_s}{4 R_{out1}} = \frac{10.6^2}{4} \cdot \frac{25\Omega}{80\Omega} \approx 9.4 \text{ dB}. \quad (8)$$

The factor of two in Eq. (7) is due to the fact that there are two mixers whose noise is uncorrelated. By substituting the data in Eq. (7) the DSB-NF of the front-end is finally given as

$$NF = 1.38 + 2 \cdot \frac{(2.36 - 1)}{8.77} \approx 2.2 \text{ dB}. \quad (9)$$

Simulations predict 2.3 dB. In addition, with the values used in this design, Eq. (5) predicts  $IIP3 \approx -16.5$  dBm for the front-end. The simulations with typical process parameters give the same result.

#### 4. LO Circuitry

The block diagram of the LO circuitry is shown in Fig. 6. The double-frequency VCO drives the flip-flops to produce the desired LO frequency with quadrature phases. The buffered LO signals drive the I and Q mixers.

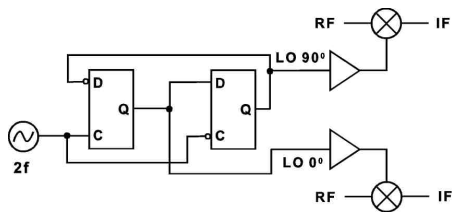


Figure 6. Block diagram of LO circuitry.

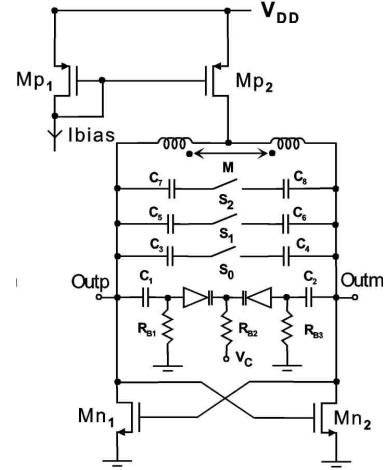


Figure 7. Schematic of VCO.

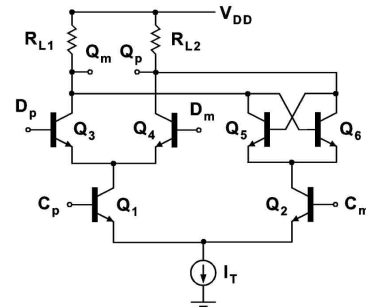


Figure 8. Schematic of flip-flop.

The VCO (Fig. 7) consists of a cross-coupled NMOS pair with a PMOS current source. A 1.5 nH differential inductor, a switchable 3-bit array of binary-weighted capacitors, and a pn-junction varactors tune the VCO to 3.15 GHz. The VCO has a continuous tuning range of 115 MHz whereas the discrete tuning scheme extends the total tuning range to 508 MHz. With the differential inductor Q of 15, the VCO output swing is about 1.8 V<sub>PP</sub> at 3 mA bias current. The source-follower buffer couples the VCO to the frequency divider.

The flip-flops (Fig. 8) use the minimum size transistors to maximize the speed with a low current consumption. The tail current is 450  $\mu$ A and the implemented bias current is inversely proportional to the reference resistor realized with the same material as the load resistors of flip-flops. This kind of biasing method minimizes the output voltage swing variations due to the variations of load resistors. The load resistors of 700  $\Omega$  set the output voltage swing to 600 mV<sub>PP</sub>.

The LO buffer consists of an emitter-follower and so-called totem-pole stage [5]. The totem-pole circuit combines the advantages of emitter-follower and common-emitter stages in the sense of charging and discharging a load capacitance. Each LO buffer is biased at the constant bias current of 850  $\mu$ A. The constant bias was found to best stabilize the LO voltage level of 500 mV<sub>PP</sub> driving the mixers.

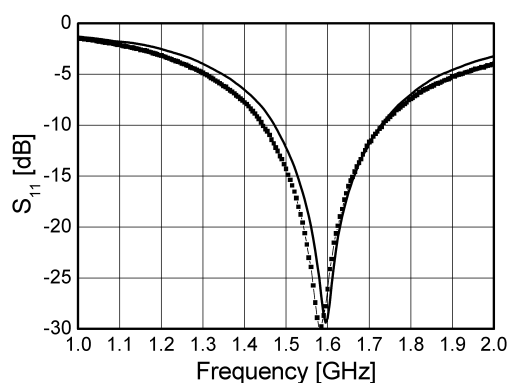


Figure 9. Measured and simulated (solid line) LNA input impedance matching.

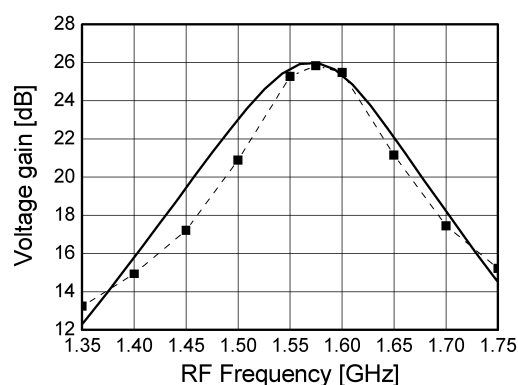


Figure 10. Measured and simulated (solid line) RF front-end voltage gain.

## 5. Measurement Results

The LNA scattering parameter  $S_{11}$  and RF front-end voltage conversion gain are plotted in Figures 9 and 10. As the mixer voltage conversion gain was designed to be 5.5 dB, the total RF front-end voltage gain is about 26 dB. The measured VCO phase noise is shown in Fig. 11. The most relevant results of the front-end are summarized in Table 1. The reported current consumption includes an LNA (2.7 mA), VCO + buffer (3.0 mA + 0.6 mA), phase shifter (1.0 mA), LO buffers (1.7 mA), and mixers (6.3 mA). The current consumption of 15.3 mA is higher than the expected 13.9 mA because the bias current used to bias the front-end was generated on-chip and this reference current varies with process.

## 6. Conclusions

A GPS direct conversion RF front-end with on-chip VCO fabricated in 0.35  $\mu\text{m}$  SiGe BiCMOS technology is presented. The equations representing the properties of

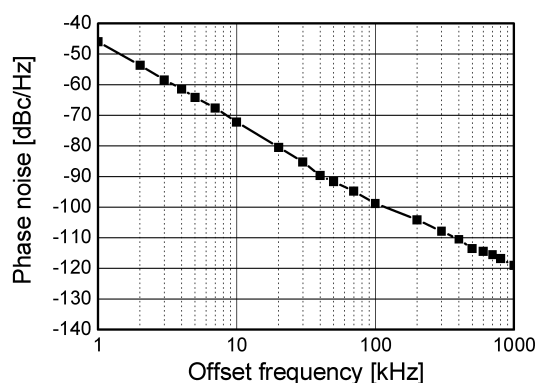


Figure 11. Measured VCO phase noise.

Table 1. RF front-end simulated and measured results.

Parameter	Sim.	Meas.	Unit
$S_{11}$ (balanced 50 $\Omega$ )	-29	$\leq -25$	dB
Voltage gain	26.0	25.8	dB
DSB-NF	2.3	2.7	dB
Phase imbalance	na	$\leq 3.0$	deg
Gain imbalance	na	0.1	dB
$P_{-1dB}$ (in-band)	-26.9	-27.6	dBm
IIP3 (in-band)	-16.5	-14.5	dBm
IIP2 (in-band)	na	+26.0	dBm
LO level at RF input	na	-105	dBm
VCO total tuning range	18	16	%
Phase noise @ 100 kHz	-94	-99	dBc / Hz
Pushing	na	-1.6	MHz / V
Current consumption	13.9	15.3	mA

the front-end are given. By applying the derived formulas, the front-end performance can be readily evaluated and optimized at the early state of the design. The results of the analysis are found to be consistent with the simulated and measured performance.

The authors wish to thank Ari Vilander, Lassi Hyvönen, and Pauli Seppinen for assistance and expertise.

## 7. References

- [1] D.K. Shaeffer, and T.H. Lee, *The Design and Implementation of Low-Power CMOS Radio Receivers*, Kluwer Academic Publishers, 1999.
- [2] H. Darabi, and A.A. Abidi, "Noise in RF-CMOS Mixers: A Simple Physical Model", *IEEE Transactions on Solid-State Circuits*, vol. 35, no. 1, January 2000.
- [3] K.L. Fong, and R.G. Meyer, "High-Frequency Nonlinearity Analysis of Common-Emitter and Differential-Pair Transconductance Stages", *IEEE Journal of Solid-State Circuits*, vol. 33, no. 4, April 1998.
- [4] B. Razavi, *RF Microelectronics*, Prentice Hall PTR, 1998.
- [5] A.S. Sedra, K.C. Smith, *Microelectronic Circuits*, Saunders College Publishing, 1989.